PHILOSOPHICAL MAGAZINE B, 2001, VOL. 81, NO. 5, 461–475

Energy spectra and photoluminescence of fractional quantum Hall systems containing a valence-band hole

ARKADIUSZ WÓJS†‡¶, KYUNG-SOO YI†§ and JOHN J. QUINN†

† University of Tennessee, Knoxville, Tennessee 37996, USA
‡ Wroclaw University of Technology, Wroclaw 50-370, Poland
§ Pusan National University, Pusan 609-735, Korea

[*Received 13 November 2000 and accepted 2 January 2001*]

ABSTRACT

The energy spectrum of a two-dimensional electron gas (2DEG) interacting with a valence-band hole is studied in the high magnetic field limit as a function of the filling factor ν and the separation d between the electron and hole layers. For d smaller than the magnetic length λ, the hole binds one or more electrons to form neutral (X) or charged (X^-) excitons. The low-lying states can be understood in terms of Laughlin-like correlations among the constituent charged fermions (electrons and X^-). For d comparable to λ, the electron–hole interaction is not strong enough to bind a full electron, and fractionally charged excitons hQE_n (bound states of a hole and one or more Laughlin quasi-electrons, QEs) are formed. The effect of these excitonic complexes on the photoluminescence spectrum is studied numerically for a wide range of values of ν and d.

§ 1. INTRODUCTION

There have been many experimental studies of photoluminescence (PL) in fractional quantum Hall systems during the past decade (Heiman *et al.* 1988, Buhmann *et al.* 1990, 1991, 1995, Goldberg *et al.* 1990, Turberfield *et al.* 1990, Goldys *et al.* 1992, Kheng *et al.* 1993, Kukushkin *et al.* 1994, Finkelstein *et al.* 1995, 1996, Shields *et al.* 1995, Brown *et al.* 1996, Gravier *et al.* 1998, Jiang *et al.* 1998, Nickel *et al.* 1998, Takeyama *et al.* 1998, Hayne *et al.* 1999, Tischler *et al.* 1999, Wojtowicz *et al.* 1999, Kim *et al.* 2000, Munteanu *et al.* 2000), but the data have been rather difficult to interpret. In order to obtain a more complete understanding of the PL process, it is essential to understand the nature of the low-energy states of the electron–hole system, and to evaluate their oscillator strength for radiative recombination. In this note we investigate the elementary excitations of a system consisting of N electrons (e) confined to the plane $z = 0$ and interacting with a single valence-band hole (h) confined to the plane $z = d$. This model is appropriate for systems in which the hole concentration is very small compared with the electron concentration so that the interaction between the holes is negligible.

There are three nearly distinct regions for the interaction of the hole and the electron system, which we refer to as weak, strong and intermediate coupling. In the weak-coupling region (d much larger than the magnetic length λ), the electron–hole

¶ Email: awojs@utk.edu

Philosophical Magazine B ISSN 1364–2812 print/ISSN 1463–6417 online © 2001 Taylor & Francis Ltd
http://www.tandf.co.uk/journals
DOI: 10.1080/13642810110036761

interaction is a weak perturbation on the eigenstates of the interacting electrons (Chen and Quinn 1993, 1994a, 1995). In the strong-coupling region ($d < \lambda$), the hole binds one or two electrons to form a neutral (X) or negatively charged (X^-) exciton (Kheng *et al.* 1993, Buhmann *et al.* 1995, Finkelstein *et al.* 1995, 1996, Hayne *et al.* 1999, Shields *et al.* 1995, Wójs and Hawrylak 1995, Palacios *et al.* 1996, Whittaker and Shields 1997, Nickel *et al.* 1998, Wójs *et al.* 1998, 1999a, b, 2000a, b, Tischler *et al.* 1999, Wojtowicz *et al.* 1999, Kim *et al.* 2000, Munteanu *et al.* 2000). When d is equal to zero, the neutral exciton is completely uncoupled from the remaining $N-1$ electrons due to the 'hidden symmetry' (Lerner and Lozovik 1981, Dzyubenko and Lozovik 1983, MacDonald and Rezayi 1990), and it is only weakly coupled at $0 < d < \lambda$. The X^- is a negatively charged fermion with a similar degenerate Landau level (LL) structure to that of an electron (Wójs and Hawrylak 1995, Wójs *et al.* 1998, 1999a). It has Laughlin-like correlations with the remaining $N-2$ electrons that can be described by a generalized composite fermion (CF) model (Wójs *et al.* 1999b). In the intermediate-coupling region ($\lambda \leq d \leq 2\lambda$), the hole can no longer bind a full electron to form an X; however, it can bind one or more Laughlin quasi-electrons (QEs) to form fractionally charged excitons, so-called FCXs (Wójs and Quinn 2001a, b). We denote a complex consisting of n QEs bound to a hole by the symbol hQE_n. To understand the stability of the hQE_n state, it is necessary to know the pseudopotentials describing the interactions of a QE–QE pair and of a h–QE pair as a function of the pair angular momentum (Wójs and Quinn 1998, 1999a, b, 2000a, Quinn and Wójs 2000). In order to determine these pseudopotentials, as well as other properties of bound complexes, we have performed exact (within the lowest LL) numerical diagonalizations for a nine-electron–one-hole system as a function of the layer separation d and the magnetic field. The calculations are performed in Haldane's spherical geometry (Haldane 1983, Fano *et al.* 1986) with the electron–hole interaction modelled by $V_{eh}(r) = e^2/(r^2 + d^2)^{1/2}$, for values of d satisfying $0 \leq d \leq 5\lambda$.

§ 2. Many-electron system

To interpret the weak-coupling regime we must begin with the understanding of an electron system in the absence of the hole. In figures 1 (*a*)–(*d*) we display the low-energy spectra of nine electrons at the LL degeneracy $g = 2S + 1$ corresponding to the magnetic monopole strength of $2S = 24$, 23, 22 and 21, respectively (on Haldane's sphere, the lowest LL is represented by a degenerate multiplet at angular momentum $l = S$). The lowest energy states contain (*a*) zero, (*b*) one, (*c*) two and (*d*) three QEs in the Laughlin $\nu = \frac{1}{3}$ state and can be simply understood using the CF picture. The effective monopole strength (Chen and Quinn 1994c, Wójs and Quinn 1998, 1999a, b, 2000a, Quinn and Wójs 2000) seen by one CF is given by $2S^* = 2S - 2(N-1)$, and the angular momentum of the kth CF shell ($k = 0, 1, \ldots$) is $l_k^* = S^* + k$. The QEs are the CFs in the first excited shell ($n = 1$) and thus have $l_{QE} = l_1^*$. The quasiholes (QHs) are the empty states in the lowest CF shell ($n = 0$) and thus have $l_{QH} = l_0^*$. For $2S = 24$ the nine CFs fill completely the $l_0^* = 4$ shell giving a total angular momentum $L_e = 0$. This non-degenerate ground state (GS) is the Laughlin incompressible $\nu = \frac{1}{3}$ state. For $2S = 23$, eight of the CFs fill the $l_0^* = \frac{7}{2}$ shell, and the ninth is a QE with $l_{QE} = \frac{9}{2}$. This gives a total angular momentum $L_e = \frac{9}{2}$ for the nine-electron GS. For $2S = 22$ we obtain two QEs each with $l_{QE} = 4$; adding the angular momenta of these two identical fermions gives $L_e = 1 \oplus 3 \oplus 5 \oplus 7$ as the low-energy band of states. For $2S = 21$ there are three

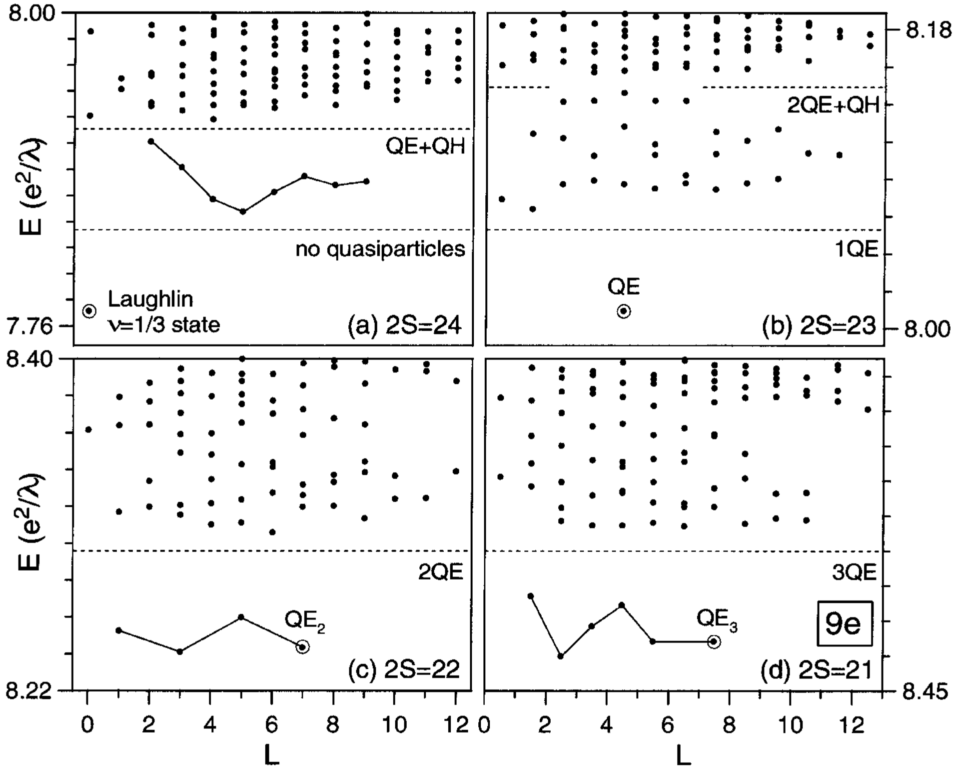

Figure 1. The energy spectra (energy E versus angular momentum L) of the nine-electron system on Haldane's sphere with the monopole strength between $2S = 24$ and 21. λ is the magnetic length.

QEs each with $l_{\mathrm{QE}} = \frac{7}{2}$. Adding their three angular momenta gives the low-lying nine-electron states at $L_{\mathrm{e}} = \frac{3}{2} \oplus \frac{5}{2} \oplus \frac{7}{2} \oplus \frac{9}{2} \oplus \frac{11}{2} \oplus \frac{15}{2}$.

In the absence of the QE–QE interaction (defined by a pseudopotential $V_{\mathrm{QE-QE}}(L)$, i.e. pair interaction energy as a function of pair angular momentum), all of the 2QE and 3QE states would be degenerate (Chen and Quinn 1994c, Sitko *et al.* 1996). However, the interaction between (charged) QEs exists and removes this degeneracy. In figure 1 (*c*), the 2QE states with $L = 3$ and 7 are lowered relative to those with $L = 1$ and 5. For the 3QE states in figure 1 (*d*), the multiplet at $L = \frac{5}{2}$ has the lowest energy and those at $L = \frac{3}{2}$ and $L = \frac{9}{2}$ have the highest energy. Remarkably, the 2QE and 3QE 'molecule' states with the maximum allowed angular momentum ($L = 2l_{\mathrm{QE}} - 1 = 7$ and $3l_{\mathrm{QE}} - 3 = \frac{15}{2}$, respectively), that is with the minimum average QE–QE separation, have low energy (Wójs and Quinn 2000b). We call these states QE_2 and QE_3.

All of the many-electron states in the lowest band can be understood on the basis of the CF picture; excellent agreement with the numerical results is obtained when interactions between quasiparticles (QP = QE or QH) are included phenomenologically (Sitko *et al.* 1996). Additionally, in many cases the first excited band of states can be identified using the CF picture. In this band, one of the CFs is excited to the next higher shell. Depending on whether a CF from the $n = 0$ or 1 shell is excited, this corresponds to the creation of an additional QE–QH pair or to the excitation of a QE with $l_{\mathrm{QE}} = l_1^*$ to the QE* state with $l_{\mathrm{QE}^*} = l_2^*$. Let us identify the first excited bands in figure 1

For $2S = 24$, no QPs occur in the lowest band, and thus the first excited band contains a single QE–QH pair. Because $l_{\mathrm{QH}} = \frac{1}{2}(N-1) = 4$ and $l_{\mathrm{QE}} = \frac{1}{2}(N+1) = 5$, the multiplets from $L = l_{\mathrm{QE}} - l_{\mathrm{QH}} = 1$ to $l_{\mathrm{QE}} + l_{\mathrm{QH}} = N = 9$ are expected for such a pair. It is known (Sitko *et al.* 1996) that the state at $L = 1$ (i.e. at the smallest average QE–QH separation) is pushed to higher energy (or forbidden) by the strong hard-core QE–QH repulsion. As a result, the 'magnetoroton' QE–QH band extends from $L = 2$ to N.

For $2S = 23$, two different QP configurations occur in the first excited band. The first consists of a single QE* with $l_{\mathrm{QE}^*} = \frac{11}{2}$ giving also the total angular momentum of $L = \frac{11}{2}$. The second consists of a single QH with $l_{\mathrm{QH}} = \frac{7}{2}$ and a pair of QEs each with $l_{\mathrm{QE}} = \frac{9}{2}$. Totally ignoring interactions between these QPs gives the following set of degenerate angular momentum multiplets for the 2QE + QH configuration: $L = \frac{1}{2} \oplus (\frac{3}{2})^2 \oplus (\frac{5}{2})^3 \oplus (\frac{7}{2})^4 \oplus (\frac{9}{2})^4 \oplus (\frac{11}{2})^4 \oplus (\frac{13}{2})^3 \oplus (\frac{15}{2})^3 \oplus (\frac{17}{2})^2 \oplus (\frac{19}{2})^2 \oplus \frac{21}{2} \oplus \frac{23}{2}$. The QP–QP interactions (particularly, the QE–QH hard-core repulsion) will remove the degeneracy of this band and push some of the multiplets into the continuum of higher energy states. However, almost all of the predicted multiplets appear in the numerical spectrum in figure 1 (*b*).

For $2S = 22$ there are again two possible configurations for the first excited band. The first contains one QE with $l_{\mathrm{QE}} = 4$ and one QE* with $l_{\mathrm{QE}^*} = 5$, and gives a band of multiplets extending from $L = 1$ to 9. The second configuration contains three QEs each with $l_{\mathrm{QE}} = 4$ and a QH with $l_{\mathrm{QH}} = 3$. Neglecting QP–QP interactions, these two QP configurations would yield a degenerate band of multiplets at $L = 0^2 \oplus 1^3 \oplus 2^5 \oplus 3^6 \oplus 4^7 \oplus 5^6 \oplus 6^7 \oplus 7^5 \oplus 8^4 \oplus 9^3 \oplus 10^2 \oplus 11 \oplus 12$. The numerical spectrum shown in figure 1 (*c*) contains many of these states in a first excited band which is rather well separated from the continuum of higher states for $L < 3$ and $L > 6$, but not well defined between these regions.

Finally, for $2S = 21$ there are two configurations for the first excited band: first with two QEs each with $l_{\mathrm{QE}} = \frac{7}{2}$ and one QE* with $l_{\mathrm{QE}^*} = \frac{9}{2}$, and second with four QEs with $l_{\mathrm{QE}} = \frac{7}{2}$ and one QH with $l_{\mathrm{QH}} = \frac{5}{2}$. The former configuration yields the set of multiplets at $L = \frac{1}{2} \oplus (\frac{3}{2})^2 \oplus (\frac{5}{2})^3 \oplus (\frac{7}{2})^3 \oplus (\frac{9}{2})^4 \oplus (\frac{11}{2})^3 \oplus (\frac{13}{2})^3 \oplus (\frac{15}{2})^2 \oplus (\frac{17}{2})^2 \oplus \frac{19}{2} \oplus \frac{21}{2}$. The latter one gives $L = (\frac{1}{2})^2 \oplus (\frac{3}{2})^4 \oplus (\frac{5}{2})^6 \oplus (\frac{7}{2})^6 \oplus (\frac{9}{2})^6 \oplus (\frac{11}{2})^5 \oplus (\frac{13}{2})^5 \oplus (\frac{15}{2})^3 \oplus (\frac{17}{2})^2 \oplus \frac{19}{2} \oplus \frac{21}{2}$. Again, we expect many of these multiplets to be pushed into the higher energy continuum by the QE–QH hard-core repulsion. From the numerical results in figure 1 (*d*), it can be seen that the first excited band is rather well defined for $L \leq \frac{3}{2}$ and for $L \geq \frac{13}{2}$, where the following multiplets occur: $L = \frac{1}{2} \oplus (\frac{3}{2})^3$ and $L = (\frac{13}{2})^6 \oplus (\frac{15}{2})^4 \oplus (\frac{17}{2})^3 \oplus (\frac{19}{2})^2 \oplus (\frac{21}{2})^2$.

§ 3. Weak-coupling regime

In the weak-coupling limit we expect to obtain fairly well defined bands for the electron–hole system by treating the interaction of the hole with the electrons as a small perturbation (Chen and Quinn 1993, 1994a, 1995). The low-energy bands are clearly visible in figure 2, and they are easily understood on the basis of figure 1 with the addition of the angular momenta of the low-energy electron multiplets to that of the hole. The angular momentum of the hole, l_{h}, is equal to S, and so $l_{\mathrm{h}} = 12, \frac{23}{2}, 11$ and $\frac{21}{2}$ in figures 1 (*a*)–(*d*), respectively. In figure 1 (*a*) the only electron multiplet in the low-energy sector is the Laughlin GS at $L_{\mathrm{e}} = 0$. Therefore, the low-energy band

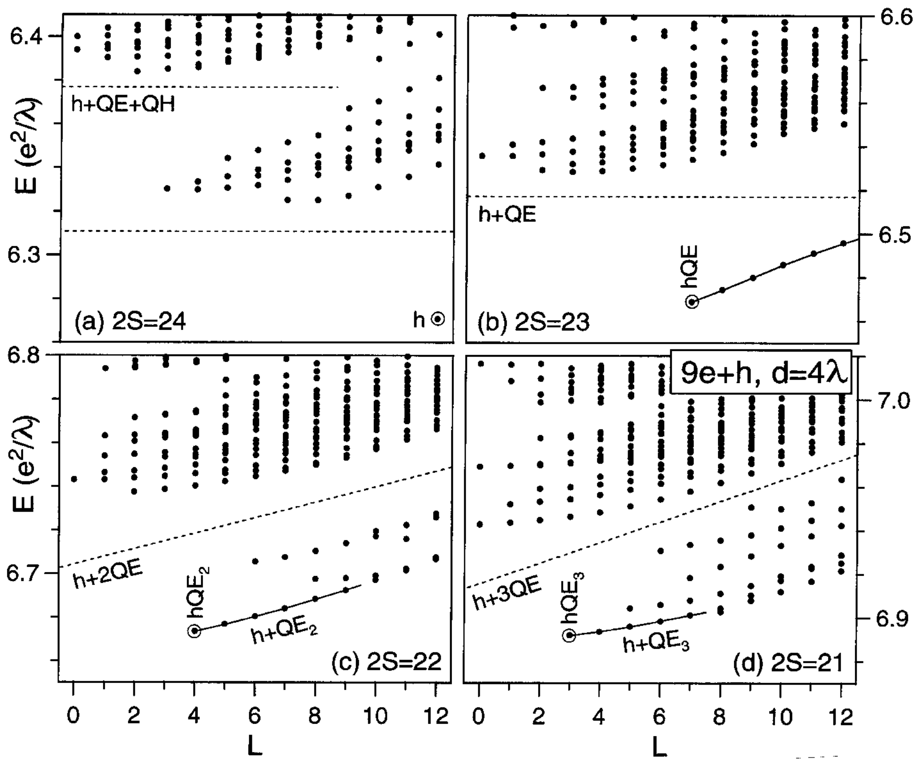

Figure 2. The energy spectra (energy E versus angular momentum L) of the nine-electron–one-hole system on Haldane's sphere with the monopole strength between $2S = 24$ and 21. The separation of electron and hole layers is $d = 4\lambda$ (weak-coupling regime). λ is the magnetic length.

in figure 2 (a) consists of a single multiplet at $L = l_h = 12$. In the other frames of figure 1, the allowed low-energy electron multiplets are those of (b) one, (c) two and (d) three QEs. When l_h is added to each of the values of L_e corresponding to a low-energy electron state, a band of multiplets is obtained with values of L satisfying $|l_h - L_e| \leq L \leq l_h + L_e$. If the separation d between electron and hole layers were infinite, so that $V_{eh} = 0$, every multiplet in a given band would be degenerate and have an energy equal to the energy of the appropriate electron state plus the (cyclotron) energy of the hole, which is a constant. The finite electron–hole interaction causes finite attraction between the hole and (negatively charged) QEs so that the energies within each band increase with increasing L (decreasing average h–QE separation). For the electronic multiplets that are close in energy, the h–QE attraction can also cause mixing or even reversing of the order of the corresponding electron–hole bands.

This very simply explains all of the electron–hole bands appearing in the low-energy sector of figure 2. For example, in figure 2 (c) there are four h+ 2QE bands starting at $L = 4$, 8, 6 and 10 resulting from the low-energy electronic states in figure 1 (c) at $L_e = 7$, 3, 5 and 1, respectively. The bands starting at $L = 4$ and 8 have lower energy than those starting at $L = 6$ and 10 because the electronic multiplets at $L_e = 7$ and 3 have lower energy than those at $L_e = 5$ and 1. For the first excited sector in figure 2, we do exactly the same thing, add l_h to the allowed values of L_e in the first excited sector of figure 1. For $2S = 24$ this gives bands beginning at $L = 3, 4, 5, \ldots, 10$, corresponding to $L_e = 9, 8, 7, \ldots, 2$. All these bands are observed in figure 2 (*a*). At $2S = 23$, there are a very large number of electronic multiplets in the first excited sector of figure 1 (*b*), but if we concentrate on the low-energy multiplets at $L_e \approx l_h = S$, which would give low-energy electron–hole bands beginning at low values of $L = |l_h - L_e|$, we would expect only a single band beginning at $L = 0$ and a single band beginning at $L = 1$, originating from the 2QE + QH multiplets at $L_e = \frac{23}{2}$ and $\frac{21}{2}$, respectively. Beginning at $L = 2$, we would expect two new bands, one at lower and one at higher energy, originating from two 2QE + QH multiplets at $L_e = \frac{19}{2}$. We would also expect one low- and one high-energy band beginning at $L = 3$ arising from the two multiplets at $L_e = \frac{17}{2}$, etc. All these bands can be identified at low L in figure 2 (*b*). For $2S = 22$ and 21, the first excited bands beginning at low values of L can be understood in exactly the same way, that is by picking out the low-energy electronic states at values of L_e close to l_h. Thus, all the low-energy electron–hole bands in figure 2 can be rather well understood in the weak-coupling limit.

Although the attraction between the hole and a given N-electron eigenstate vanishes in the $d \to \infty$ limit, the most tightly bound states of a hole and one, two and three QEs can be identified in figure 2. In these states, denoted as hQE, hQE_2 and hQE_3, a QE or an appropriate QE molecule moves as close to the hole as possible. These states have the smallest L within their h+ QE, h+ QE_2 or h+ QE_3 bands and, together with the 'uncoupled-hole' state h in figure 2 (*a*), are the elementary excitations of the weak-coupling regime at finite d.

§ 4. Strong-coupling regime

In the strong-coupling regime the hole binds one or two electrons to form an X or an X^-. For $d = 0$, the X is totally uncoupled from the remaining $N - 1$ electrons (Lerner and Lozovik 1981, Dzyubenko and Lozovik 1983, MacDonald and Rezayi 1990) and it is only weakly coupled if d is small compared to λ. In contrast, the X^- is a negatively charged fermion with LL structure just like an electron (Wójs and Hawrylak 1995, Wójs *et al.* 1998, 1999a). Because the e–X^- pseudopotential rises more quickly with pair angular momentum than the harmonic pseudopotential (Wójs and Quinn 1998, 1999a, b, 2000a, Quinn and Wójs 2000) the low-energy states of the X^- and $N_e = N - 2$ remaining electrons can be described by the generalized CF picture (Wójs *et al.* 1999b) which accounts for Laughlin-like correlations among the two types of constituent charged particles.

For the system containing one X^- and N_e remaining electrons, the effective monopole strengths seen by an electron is given by (Wójs *et al.* 1999b)

$$2S_e^* = 2S - (m_e - 1)(N_e - 1) - m_{eX^-}, \tag{1}$$

while that seen by an X^- is

$$2S_{X^-}^* = 2S - m_{eX^-} N_e. \tag{2}$$

Here m_{eX^-} is the exponent describing the Laughlin correlations between the X^- and each electron in the two-component many-body wavefunction. In the generalized CF picture, electrons and X^-'s are converted into two types of CFs: CF-e and CF-X^-. The angular momenta of their lowest shells are $l_e^* = S_e^*$ and $l_{X^-}^* = S_{X^-}^* - 1$. The following types of Laughlin QPs can be defined: the particles in the first excited

CF-e shell are 'e-type' quasi-electrons (QE-e) with $l_{\mathrm{QEe}} = l_{\mathrm{e}}^{*} + 1$, the empty states in the lowest CF-e shell are 'e-type' quasiholes (QH-e) with $l_{\mathrm{QHe}} = l_{\mathrm{e}}^{*}$, and a single particle in the lowest CF-X^{-} shell is an 'X^{-}-type' quasi-electron (QE-X^{-}) with $l_{\mathrm{QEX^-}} = l_{\mathrm{X^-}}^{*}$. For simplicity, in the figures we denote QH-e and QE-X^{-} by QH and X^{-}, respectively.

Let us turn to the nine-electron–one-hole spectra shown in figure 3. For $2S = 21$, the energies of the multiplicative states (containing one uncoupled X) are exactly the same as those of eight electrons, with the energy shifted by the X binding energy. For the eight electrons, the lowest CF shell has $l_0^{*} = \frac{7}{2}$, and it is filled completely giving an $L = 0$ Laughlin GS. An excitation of one CF to the next shell gives a 'magnetoroton' QE–QH band extending from $L = 2$ to 8, marked with a dashed line. The lowest non-multiplicative states contain seven electrons and an X^{-}. For $m_{\mathrm{e}} = 3$ and $m_{\mathrm{eX^-}} = 2$ we obtain $2S_e^{*} = 2S_{\mathrm{X^-}}^{*} = 7$. The eight states in the lowest CF-e shell contain one QH-e with $l_{\mathrm{QHe}} = \frac{7}{2}$, and the single QE-$X^{-}$ has $l_{\mathrm{QEX^-}} = \frac{5}{2}$. The addition of l_{QHe} and $l_{\mathrm{QEX^-}}$ gives the band of multiplets extending from $L = 1$ to 6. These states are the bound states of a QH-e–QE-X^{-} pair, connected by a solid line in figure 3 (*d*). Their energy increases with increasing L, just as that of the neutral exciton does. Our interpretation of this low-lying band of non-multiplicative states is totally different from that of a neutral exciton with finite momentum which is dressed by magneto-

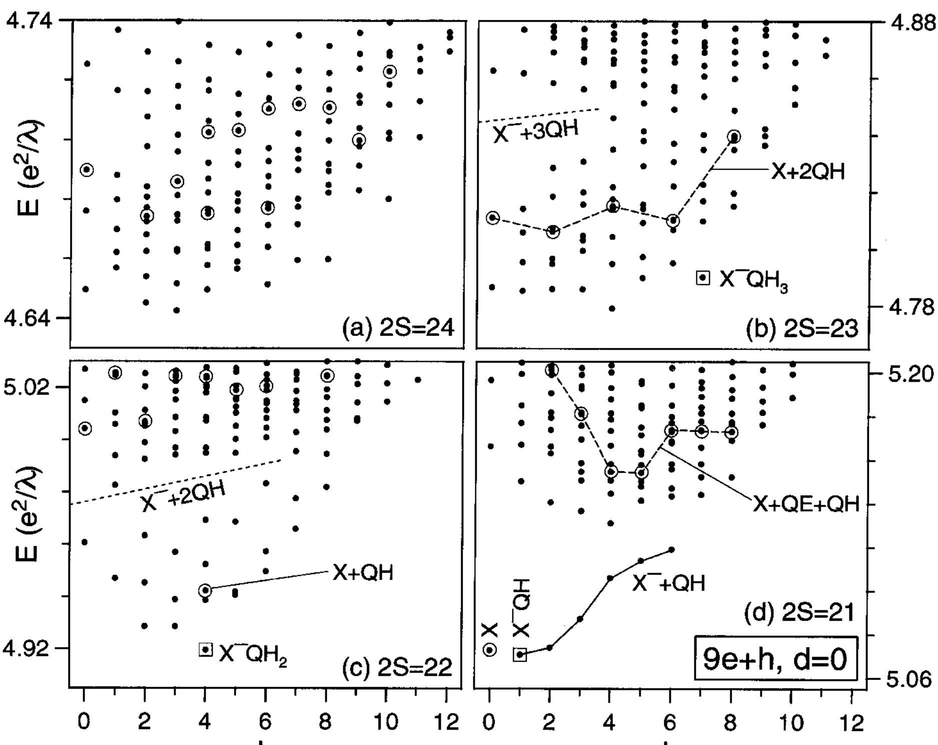

Figure 3. The energy spectra (energy E versus angular momentum L) of the nine-electron–one-hole system on Haldane's sphere with the monopole strength between $2S = 24$ and 21. The separation of electron and hole layers is $d = 0$ (strong-coupling regime). λ is the magnetic length.

rotons of the Laughlin condensed state, suggested by previous authors (Apalkov and Rashba 1992, 1993, MacDonald *et al.* 1992, Wang *et al.* 1992). The latter picture does not work because the coupling of an exciton with a finite electric dipole moment to the electrons is too strong to be treated perturbatively.

For $2S = 22$, there is a single low-energy multiplet at $L = 4$ that is a multiplicative state. It corresponds to a single QH in the l_0^* shell. The non-multiplicative states exhibit a low-energy band containing the multiplets at $L = 0 \oplus 1 \oplus 2^3 \oplus 3^3 \oplus 4^4 \oplus 5^3 \oplus 6^3 \oplus 7^2 \oplus 8^2 \oplus 9 \oplus 10$. These arise from two QH-e's each with $l_{\mathrm{QHe}} = 4$ plus one QE-X$^-$ with $l_{\mathrm{QEX}^-} = 3$. The GS called X$^-$QH$_2$ marked with an open square is the most tightly bound state of QE-X$^-$ and a (QH-e)$_2$ molecule. Its angular momentum $L = 4$ results from adding two l_{QHe}'s to obtain $l_{(\mathrm{QHe})_2} = 2l_{\mathrm{QHe}} - 1 = 7$, and then adding to it one l_{QEX^-} to obtain $l_{\mathrm{X^-QH_2}} = |l_{\mathrm{QEX}^-} - l_{(\mathrm{QH}e)_2}| = 4$.

For $2S = 23$, the low-energy band of multiplicative states contains two QHs each with $l_{\mathrm{QH}} = \frac{9}{2}$, resulting in the multiplets $L = 0 \oplus 2 \oplus 4 \oplus 6 \oplus 8$ (connected with a dashed line). The non-multiplicative states have a low-energy band containing three QH-e's each with $l_{\mathrm{QHe}} = \frac{9}{2}$ and one QE-X$^-$ with $l_{\mathrm{QEX}^-} = \frac{7}{2}$. Addition of these angular momenta gives a band of multiplets at $L = 0 \oplus 1^4 \oplus 2^6 \oplus 3^7 \oplus 4^8 \oplus 5^9 \oplus 6^8 \oplus 7^8 \oplus 8^7 \oplus 9^5 \oplus 10^4 \oplus 11^3 \oplus 12^2 \oplus 13 \oplus 14$. The angular momentum of the most tightly bound state of a QE-X$^-$ and a (QH-e)$_3$ molecule is $l_{\mathrm{X^-QH_3}} = 7$. This state is (most likely) the one marked with an open rectangle.

Finally, for $2S = 24$ the low-lying band of multiplicative state contains $L = 0 \oplus 2 \oplus 3 \oplus 4^2 \oplus 5 \oplus 6^2 \oplus 7 \oplus 8 \oplus 9 \oplus 10 \oplus 12$, arising from three QHs each with $l_{\mathrm{QH}} = 5$. The lowest non-multiplicative band contains four QH-e's each with $l_{\mathrm{QHe}} = 5$ and one QE-X$^-$ with $l_{\mathrm{QHX}^-} = 4$. It produces 194 multiplets starting with $L = 0^3 \oplus 1^6 \oplus \ldots$ and ending with $15^3 \oplus 16^2 \oplus 17 \oplus 18$. Only the lower-energy multiplets of this set are shown in figure 3 (*d*) in which we have restricted the range of energy and L.

It is really quite remarkable that the myriad of multiplets associated with the lowest band of both multiplicative and non-multiplicative states appear in the numerical spectra shown in figure 3 exactly as predicted by the generalized CF picture. This simple model ignores the interaction between QPs which can lead to some overlap of the lowest bands with higher bands at some values of L when the QP–QP interaction energy becomes large.

§ 5. Intermediate-coupling regime

When the separation d increases beyond roughly one magnetic length λ, the attractive Coulomb potential of the hole is not strong enough (and its resolution is not high enough) to bind a full electron. We know this from numerical calculations for a single electron and hole as a function of d at different values of $2S$. When many electrons are present, it is possible that the X and even the X$^-$ may persist to larger values of d due to correlations within the entire electron system. However, from knowing that at large values of d, V_{eh} acts as a small perturbation on the N-electron eigenstates, we might guess that Laughlin QEs rather than 'full' electrons could bind to the hole to form FCXs. The prediction that QEs can bind to a hole at $d > \lambda$ at which 'full' electrons do not is based on two simple facts: (i) negative electric charge of QEs ($q_{\mathrm{QE}} = -\frac{1}{3}e$ at $\nu = \frac{1}{3}$) causes h–QE attraction and (ii) because the number of QEs is smaller than the number of electrons, their characteristic separation is larger and their interaction energy is smaller than those of electrons, and thus smaller strength and lower resolution of the hole's attractive potential are sufficient to pick one out of many interacting QEs to form a bound state.

In figures 4 and 5 we present the spectra obtained for the nine-electron–one-hole system at $d = \lambda$ and 2λ. We shall attempt to interpret the low-lying bands in terms of the elementary excitations and their interactions. Because $d = \lambda$ and 2λ are on the borders of strong- and weak-coupling regions, respectively, the interpretation is not always unique. The stable elementary excitations of the strong-coupling regime are X, X^-, X^-QH or X^-QH_2, and those of the weak-coupling regime are h, hQE and hQE_2. At the values of $2S = 21$ and 24, at which the lowest-lying states or bands at small and large d occur at different L, the d-driven phase transition between the two regimes is of first order and the crossing of the appropriate energy levels is observed in the spectrum. However, this is not the case for $2S = 22$ where X^-QH_2 has the same $L = \frac{1}{2}(N - 1)$ as hQE_2, or at $2S = 23$ where X^-QH_3 has the same $L = N - 2$ as hQE. In these spectra, the anti-crossing of energy levels occurs, and the analysis of wavefunctions is needed to detect the phase transition (of the second order) between the two regions.

For $2S = 21$, it is clear from figures 4 (d) and 5 (d) that the band of states extending from $L = 0$ to 6 appearing in figure 3 (d) is still present beyond $d = \lambda$. For $L = 5$ and 6 it crosses into the continuum of higher energy states. For $d = 0$, this band was identified as the multiplicative state of eight electrons in a Laughlin

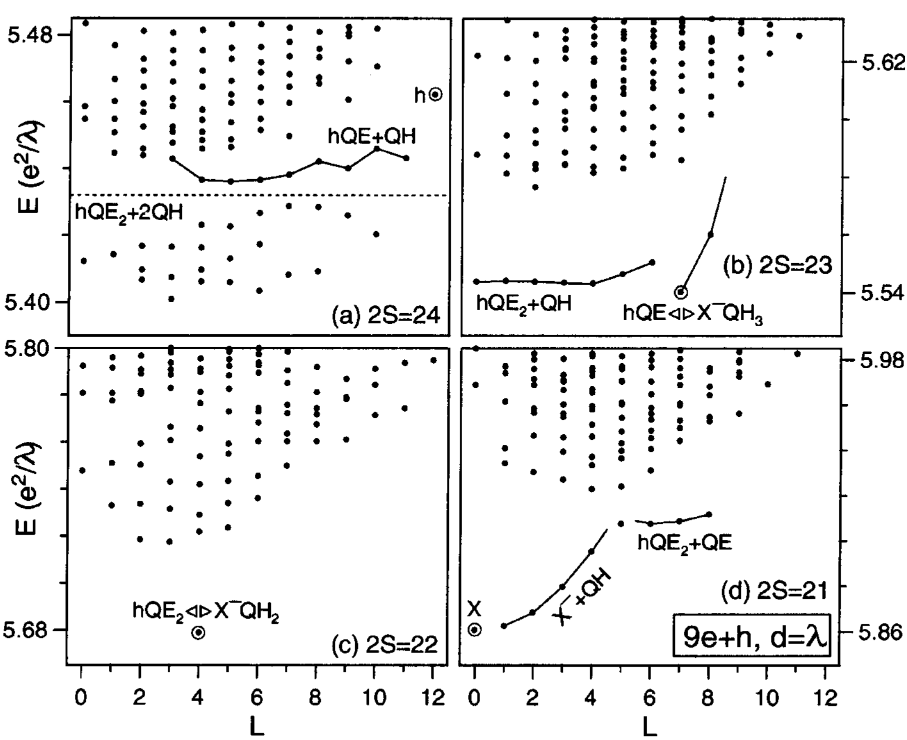

Figure 4. The energy spectra (energy E versus angular momentum L) of the nine-electron–one-hole system on Haldane's sphere with the monopole strength between $2S = 24$ and 21. The separation of electron and hole layers is $d = \lambda$ (intermediate-coupling regime). λ is the magnetic length.

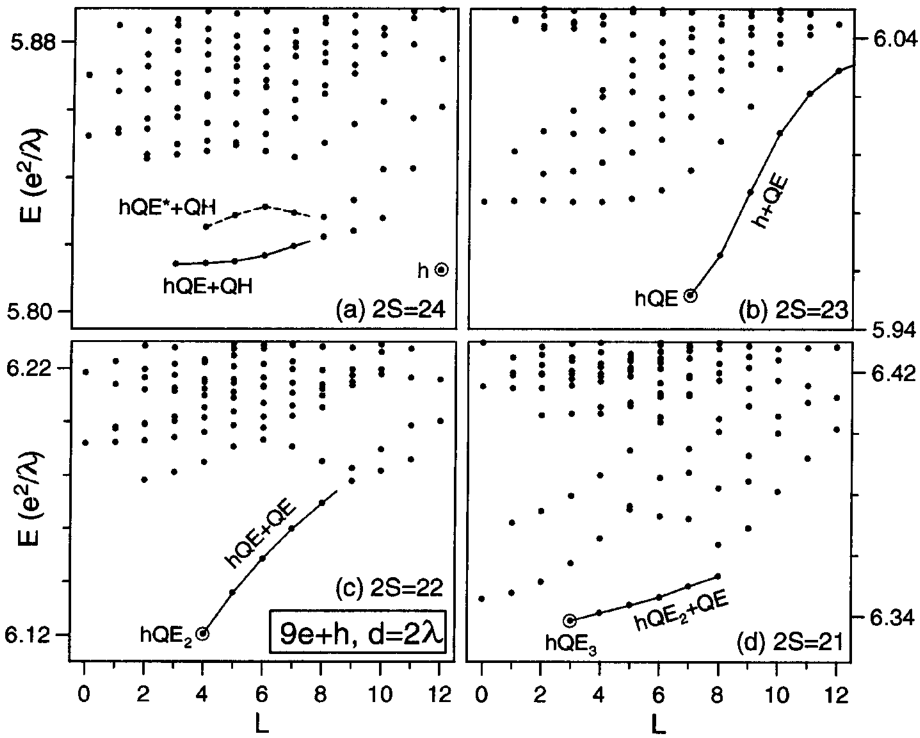

Figure 5. The energy spectra (energy E versus angular momentum L) of the nine-electron–one-hole system on Haldane's sphere with the monopole strength between $2S = 24$ and 21. The separation of electron and hole layers is $d = 2\lambda$ (intermediate-coupling regime). λ is the magnetic length.

incompressible state plus an X in its GS at $L = 0$ and the X^-QH band predicted by the generalized CF picture at $L = 1, 2, \ldots, 6$. Hence, we conclude that the X and X^- bound states persist beyond $d = \lambda$ in this system. The band of states extending to $L = 8$ which crosses the X^-QH band at $L = 5$ can be associated with a bound state of the hole and two Laughlin QEs, interacting with a third QE. The hQE_2 is the most strongly bound FCX, as we shall see later in this section. Since the Laughlin QE has $l_{QE} = l_1^* = S - (N-1) + 1 = \frac{7}{2}$, the allowed values of L_{2QE} are $0 \oplus 2 \oplus 4 \oplus 6$. The 2QE state with the smallest average QE–QE separation is the QE_2 molecule with $l_{QE_2} = 6$, and the hQE_2 state has $l_{hQE_2} = |l_h - l_{QE_2}| = \frac{9}{2}$. Adding to l_{hQE_2} the angular momentum of the third QE as if it were distinguishable from the two QEs within the hQE_2 would give a band of states extending from $L = |l_{hQE_2} - l_{QE}| = 1$ to $l_{hQE_2} + l_{QE} = 8$. However, the three QEs in the $hQE_2 + QE$ band are identical fermions and must obey and the Pauli exclusion principle. The exclusion principle forbids a number of $hQE_2 + QE$ pair states corresponding to the smallest hQE_2–QE separation. The forbidden states can be most easily identified by noticing that the largest angular momentum of three QEs is $l_{QE_3} = 3l_{QE} - 3 = \frac{15}{2}$ which, when added to $l_h = \frac{21}{2}$, cannot result in a total h+ 3QE angular momentum smaller than 3. Thus, the $L = 1$ and 2 states of the hQE_2–QE pair are forbidden and the hQE_2–QE band is expected to extend from $L = 3$ to 8, exactly as observed in figure 5 (d). Remarkably, although the hQE_2 and QE have opposite charges ($q_{hQE_2} = +\frac{1}{3}e$ and $q_{QE} = -\frac{1}{3}e$), the interaction energy does not increase with increasing L as it does for the electron–hole pair. This is due to the complex (not point particle) structure of the constituents, which makes the hQE_2–QE interaction not generally attractive (and is responsible for the instability of the hQE_3 complex). In figure 5 (*d*), the entire hQE_2 band at $L = 3$ to 8 is observed at $d = 2\lambda$, as it is lower in energy that the remnants of the X^-–QH band.

For $2S = 22$, a second-order transition between the X^-QH_2 GS of the strong coupling at $L = 4$ and the hQE_2 GS of the weak coupling at the same L is observed in figures 4 (*c*) and 5 (*c*). Although it is not clear from the energy spectrum alone, the two GSs anti-cross at $d \approx \lambda$. The low-lying excitations of the hQE_2 state at $d = 2\lambda$ are connected with a solid line in figure 5 (*c*). At this intermediate value of d, they are best interpreted as a dispersion of a hQE–QE pair. This changes at larger d when the QE–QE interaction becomes dominant over the hQE–QE interaction and the low-lying excitations of the hQE_2 state turn into the h–QE_2 pair excitations identified in figure 2 (*c*).

For $2S = 23$, a similar second-order transition between the X^-QH_3 and hQE states occurs at $L = 7$. Additionally, a well-defined band of hQE_2–QH pair states occurs at $L = 0$ to 6. This band occurs only in the intermediate-coupling region (at $d \approx \lambda$) and cannot be found in figure 2 or 3. The range of d in which it has low energy is determined by the competition between the hQE–QE binding energy gained through the formation of a hQE_2 state and the Laughlin energy gap to create an additional QE–QH pair. The angular momenta of the hQE_2–QH states result from adding $l_{hQE_2} = \frac{7}{2}$ to $l_{QH} = \frac{7}{2}$ to obtain $L = 0$ to 7. The $L = 7$ state corresponding to the smallest average hQE_2–QH separation is most likely pushed to a high energy because of the QE–QH hard core.

Finally, at 2S= 24 the lowering of energy of the h state at $L = 12$ with increasing d is observed. In this state the hole becomes completely uncoupled from the nine-electron Laughlin GS in the $d \to \infty$ limit. Other low-energy bands that occur in the intermediate-coupling regime involve one or two QE–QH pairs spontaneusly induced in the electron system to screen the charge of the hole. At a smaller $d = \lambda$, the coupling of the hole to the Laughlin excitations of the electron GS is stronger and the $hQE_2 + 2QH$ band has the lowest energy. At a larger $d = 2\lambda$, the coupling is weaker (and so is the h–QE attraction compared to the Laughlin gap) and the band of hQE–QH pair states at $L = 3$ to 11 moves down in energy relative to the $hQE_2 + 2QH$ band. The band starting at $L = 4$ and going slightly above the hQE–QH band is best interpreted as the band of hQE*–QH states in which hQE* is the first excited state of hQE, with the angular momentum $l_{hQE^*} = l_{hQE} + 1$. As shown in figure 2 (*a*), at even higher d, when the distant hole uncouples from the electron system, all bands involving QE–QH pairs reconstruct and the h GS becomes stable. The angular momenta of the hQE–QH and hQE*–QH pairs can be calculated by adding $l_{hQE} = 7$ or $l_{hQE^*} = 8$ to $l_{QH} = 4$ to obtain $L = 3$ to 11 and $L = 4$ to 12, respectively. For the $hQE_2 + 2QH$ band, $l_{hQE_2} = 3$ must be added to all possible values of $L_{2QH} = 1 \oplus 3 \oplus 5 \oplus 7$. The result is $L = 0 \oplus 1 \oplus 2^3 \oplus 3^3 \oplus 4^4 \oplus 5^3 \oplus 6^3 \oplus 7^2 \oplus 8^2 \oplus 9 \oplus 10$; all these multiplets occur below the dotted line in figure 4 (*a*).

§ 6. Photoluminescence

In the preceding sections we have identified the low-lying elementary excitations of an ideal system containing N electrons confined to a plane and one hole confined to a neighbouring parallel plane in the high magnetic field limit. In this limit the cyclotron energy $\hbar\omega_c$ is so large compared with the Coulomb energy e^2/λ that only the lowest LL need be considered (Wójs and Quinn 2001a, b). In actual experiments at finite magnetic fields, the mixing of LLs by the Coulomb interaction occurs. It is particularly important in the strong-coupling regime. While only one bound X^- state exists in the lowest LL—the non-radiative triplet (Wójs and Hawrylak 1995, Palacios *et al.* 1996) with parallel electron spins identified in figure 3—the LL mixing leads to the binding of other X^- states, particularly of the optically active singlet (Buhmann *et al.* 1995, Kheng *et al.* 1993, Whittaker and Shields 1997, Wójs *et al.* 2000a, b) observed in PL. The LL mixing is less important for the intermediate and weak coupling. Real systems are also complicated by finite quantum well widths, different barrier heights for electrons and holes, non-parabolicity of the energy bands, spin–orbit coupling, etc.

In this section we will discuss PL (radiative recombination of an electron–hole pair) in the 'theoretical' situation in which the interacting particles are confined to planes and only the lowest LL is taken into account ($B \to \infty$). There are two symmetries that limit the possible radiative decay processes (Wójs and Quinn 2000a, b, 2001a, b). The most important one is the geometrical symmetry: translational invariance on a plane (or rotational invariance on Haldane's sphere). On the plane there are two conserved orbital quantities $\mathcal{M}$, the z component of angular momentum, and $\mathcal{K}$, an additional quantum number associated with the partial decoupling of the centre-of-mass motion of the electron–hole system in the magnetic field (Avron *et al.* 1978, Dzyubenko 2000). States in a given LL all have the same value of $\mathcal{L} = \mathcal{M} + \mathcal{K}$, and different states in a LL are labelled by $\mathcal{K} = 0, 1, 2, \ldots$. On the spherical surface, the total angular momentum L and its z component L_z are conserved. The other symmetry is the 'hidden symmetry' which is exact in the lowest LL at $d = 0$ and only weakly broken in the entire weak-coupling regime. The 'hidden symmetry', that is the particle–hole symmetry of the electron–valence-band-hole Hamiltonian H, depends on equal magnitude of the electron–electron and electron–hole interactions in the lowest LL. This symmetry makes the commutator of the PL operator $\mathcal{P}$ which annihilates an optically active electron–hole pair with H proportional to $\mathcal{P}$ itself (Dzyubenko and Lozovik 1983, MacDonald and Rezayi 1990). Because of this, only the multiplicative states (containing one uncoupled neutral exciton) are radiative at $d = 0$. At $d > 0$, the states originating from other, non-multiplicative states become radiative, but their PL intensity remains very low at $d < \lambda$. Thus the PL spectrum in the weak-coupling regime gives information about the binding of the X, but not about original electron–electron correlations in the two-dimensional electron gas (2DEG).

For weak and intermediate coupling the system is best described in terms of the hQE_n bound states (FCXs). At $\nu \approx \frac{1}{3}$, the recombination process can be thought of as (Chen and Quinn 1994b)

$$h + nQE \to (3 - n)QH + \gamma. \tag{3}$$

In other words, the hole plus $n = 0$, 1, 2 or 3 Laughlin QEs combine to give off a photon γ plus $3 - n = 3$, 2, 1 or 0 Laughlin QEs. Other processes, involving additional QE–QH pairs, have much smaller oscillator strength. In figure 2 we have shown the low-lying bands for the nine-electron–one-hole systems that contain (*a*) zero, (*b*) one, (*c*) two and (*d*) three QEs, respectively. At zero temperature only the lowest state in each frame is occupied and can serve as an initial state. At finite temperature T, the probability of the eigenstate of energy E being occupied is proportional to $\exp[-E/k_B T]$. The PL spectra are obtained by evaluating the transition rate $w_{i\to f}$ between low-lying initial states $|i\rangle$ of the N-electron–one-hole system and final states $|f\rangle$ of the $(N-1)$-electron system,

$$w_{i\to f} = \text{const} \times |\langle f|\mathcal{P}|i\rangle|^2. \tag{4}$$

We have used the eigenfunctions of the nine-electron–one-hole system and of the eight-electron system obtained in numerical diagonalization to evaluate $w_{i\to f}$. We find the following results for weak and intermediate coupling (Wójs and Quinn 2001a, b).

(i) For weak coupling, the PL intensity is weak. However, the PL spectra can involve one or more peaks of different relative intensities whose energies depend on the value of n in equation (3).

(ii) For intermediate coupling, the strongest emission is that of the strongly bound and radiative hQE_2. The recombination of the hQE ground state is forbidden by the conservation of L (or $\mathcal{K}$), but the excited state hQE* is radiative. The 'uncoupled-hole' state h is radiative and, finally, the hQE_3 'anyon exciton' proposed earlier (Rashba and Portnoi 1993) is neither bound nor radiative.

Let us illustrate the $\Delta L = 0$ optical selection rule on the examples of the hQE_2 and hQE recombination. An isolated hQE_2 state occurs in the nine-electron–one-hole system at $2S = 22$; see figure 5 (*c*). Its angular momentum, $l_{hQE_2} = 4$, arose from $l_{QE} = 4$ and $l_{QE_2} = 7$ combined with $l_h = 11$. After the recombination, we are left with one QH in the eight-electron system, which has the same angular momentum, $l_{QH} = S^* = 4$. Therefore, $|i\rangle = |hQE_2\rangle$ and $|f\rangle = |QH\rangle$ each have $L = 4$, and the optical process is allowed by the $\Delta L = 0$ selection rule.

The isolated hQE and hQE* states occur at $2S = 23$; see figure 5 (*b*). Their angular momenta, $l_{hQE} = 7$ and $l_{hQE^*} = 8$, resulted from $l_{QE} = \frac{9}{2}$ combined with $l_h = \frac{23}{2}$. In the final state, two QHs occur each with $l_{QH} = \frac{9}{2}$. The allowed angular momenta for the 2QH pair states are $L_{2QH} = 0 \oplus 2 \oplus 4 \oplus 6 \oplus 8$. Comparing angular momenta of initial and final states we obtain that the $|i\rangle = |hQE\rangle$ initial ground state cannot recombine to create a 2QH pair, $|f\rangle = |2QH\rangle$. However, the excited initial state $|i\rangle = |hQE^*\rangle$ is optically active, and the final state for its recombination is the $|f\rangle = |QH_2\rangle$ molecule. Because hQE* is an excited state, its PL line is expected at $T > 0$.

§ 7. Summary

We have calculated numerically the exact eigenstates of the nine-electron–one-hole system on Haldane's sphere in the 'ideal' theoretical limit of $\hbar\omega_c \to \infty$ and zero widths of electron and hole layers. We have shown how the low-lying bands in strong, weak and intermediate coupling can be understood in terms of rather simple elementary composite particles (X, X^-, hQE, hQE_2, etc.) and electrons. We have studied the oscillator strength for radiative recombination and found that certain radiative decay processes are strongly inhibited. In the strong-coupling region, only the multiplicative states (or, at finite but small values of d, the states arising from them) have appreciable oscillator strength. For intermediate and strong coupling the recombination of the hQE_2 bound state has the highest intensity. The 'uncoupled hole' h and the excited state hQE* are also radiative, but the recombination of the latter state will only be observed if this state is occupied at a finite temperature at which the PL experiment is performed.

Acknowledgements

The authors thank Izabela Szlufarska for help on this problem, and acknowledge the support of the Materials Research Program of Basic Energy Sciences, US Department of Energy. A. W. acknowledges discussions with P. Hawrylak (IMS NRC Ottawa) and M. Potemski (HMFL Grenoble), and partial support of KBN Grant 2P03B05518. K.-S. Y. acknowledges support from the Korea Research Foundation.

References

Apalkov, V. M., and Rashba, E., 1992, *Phys. Rev.* B, **46**, 1628; 1993, *Phys. Rev.* B, **48**, 18312.
Avron, J. E., Herbst, I. W., and Simon, B., 1978, *Ann. Phys.*, **114**, 431.
Brown, S. A., Young, J. F., Brum, J. A., Hawrylak, P., and Wasilewski, Z., 1996, *Phys. Rev.* B, **54**, R11082.
Buhmann, H., Joss, W., von Klitzing, K., Kukushkin, I. V., Martinez, G., Plaut, A. S., Ploog, K., and Timofeev, V. B., 1990, *Phys. Rev. Lett.*, **65**, 1056.
Buhmann, H., Joss, W., von Klitzing, K., Kukushkin, I. V., Martinez, G., Ploog, K., and Timofeev, V. B., 1991, *Phys. Rev. Lett.*, **66**, 926.
Buhmann, H., Mansouri, L., Wang, J., Beton, P. H., Mori, N., Heini, M., and Potemski, M., 1995, *Phys. Rev.* B, **51**, 7969.
Chen, X. M., and Quinn, J. J., 1993, *Phys. Rev. Lett.*, **70**, 2130; 1994a, *Phys. Rev.* B, **50**, 2354; 1994b, *Solid state Commun.*,**90**, 303; 1994c, *Solid state Commun.*, **92**, 865; 1995, *Phys. Rev.* B, **51**, 5578.
Dzyubenko, A. B., 2000, *Solid state Commun.*, **113**, 683.
Dzyubenko, A. B., and Lozovik, Yu. E., 1983, *Fiz. Tverd. Tela*, **25**, 1519 [1983, *Sov. Phys. solid State*, **25**, 874].
Fano, G., Ortolani, F., and Colombo, E., 1986, *Phys. Rev.* B, **34**, 2670.
Finkelstein, G., Shtrikman, H., and Bar-Joseph, I., 1995, *Phys. Rev. Lett.*, **74**, 976; 1996, *Phys. Rev.* B, **53**, R1709.
Goldberg, B. B., Heiman, D., Pinczuk, A., Pfeiffer, L. N., and West, K., 1990, *Phys. Rev. Lett.*, **65**, 641.
Goldys, E. M., Brown, S. A., Davies, A. G., Newbury, R., Clark, R. G., Simmonds, P. E., Harris, J. J., and Foxon, C. T., 1992, *Phys. Rev.* B, **46**, R7957.
Gravier, L., Potemski, M., Hawrylak, P., and Etienne, B., 1998, *Phys. Rev. Lett.*, **80**, 3344.
Haldane, F. D. M., 1983, *Phys. Rev. Lett.*, **51**, 605.
Hayne, M., Jones, C. L., Bogaerts, R., Riva, C., Usher, A., Peeters, F. M., Herlach, F., Moshchalkov, V. V., and Henini, M., 1999, *Phys. Rev.* B, **59**, 2927.
Heiman, D., Goldberg, B. B., Pinczuk, A., Tu, C. W., Gossard, A. C., and English, J. H., 1988, *Phys. Rev. Lett.*, **61**, 605.
Jiang, Z. X., McCombe, B. D., and Hawrylak, P., 1998, *Phys. Rev. Lett.*, **81**, 3499.
Kheng, K., Cox, R. T., d'Aubigne, Y. M., Bassani, F., Saminadayar, K., and Tatarenko, S., 1993, *Phys. Rev. Lett.*, **71**, 1752.
Kim, Y., Munteanu, F. M., Perry, C. H., Rickel, D. G., Simmons, J. A., and Reno, J. L., 2000, *Phys. Rev.* B, **61**, 4492.
Kukushkin, I. V., Haug, R. J., von Klitzing, K., Eberl, K., and Töttemeyer, K., 1994, *Phys. Rev.* B, **50**, 11259.
Lerner, I. V., and Lozovik, Yu. E., 1981, *Zh. Eksp. Teor. Fiz.*, **80**, 1488 [1981, *Sov. Phys. JETP,* **53**, 763].
MacDonald, A. H., and Rezayi, E. H., 1990, *Phys. Rev.* B, **42**, 3224.
MacDonald, A. H., Rezayi, E. H., and Keller, D., 1992, *Phys. Rev. Lett.*, **68**, 1939.
Munteanu, F. M., Kim, Y., Perry, C. H., Rickel, D. G., Simmons, J. A., and Reno J. L., 2000, *Phys. Rev.* B, **61**, 4731.

Nickel, H. A., Herold, G. S., Yeo, T., Kioseoglou, G., Jiang, Z. X., McCombe, B. D., Petrou, A., Broido, D., and Schaff, W., 1998, *Phys. status solidi* B, **210**, 341.

Palacios, J. J., Yoshioka, D., and MacDonald, A. H., 1996, *Phys. Rev.* B, **54**, 2296.

Quinn, J. J., and Wójs, A., 2000, *J. Phys. condens. Matter*, **12**, R265.

Rashba, E. I., and Portnoi, M. E., 1993, *Phys. Rev. Lett.*, **70**, 3315.

Shields, A. J., Pepper, M., Simmons, M. Y., and Ritchie, D. A., 1995, *Phys. Rev.* B, **52**, 7841.

Sitko, P., Yi, S. N., Yi, K. S., and Quinn, J. J., 1996, *Phys. Rev. Lett.*, **76**, 3396.

Takeyama, S., Kunimatsu, H., Uchida, K., Miura, N., Karczewski, G., Jaroszynski, J., Wojtowicz, T., and Kossut, J., 1998, *Physica* B, **246–247**, 200.

Tischler, J. G., Weinstein, B. A., and McCombe, B. D., 1999, *Phys. status solidi* B, **215**, 263.

Turberfield, A. J., Haynes, S. R., Wright, P. A., Ford, R. A., Clark, R. G., Ryan, J. F., Harris, J. J., and Foxon, C. T., 1990, *Phys. Rev. Lett.*, **65**, 637.

Wang, B. S., Birman, J. L., and Su, Z. B., 1992, *Phys. Rev. Lett.*, **68**, 1605.

Whittaker, D. M., and Shields, A. J., 1997, *Phys. Rev.* B, **56**, 15185.

Wojtowicz, T., Kutrowski, M., Karczewski, G., Kossut, J., Teran, F. J., and Potemski, M., 1999, *Phys. Rev.* B, **59**, R10437.

Wójs, A., and Hawrylak, P., 1995, *Phys. Rev.* B, **51**, 10880.

Wójs, A., Hawrylak, P., and Quinn, J. J., 1998, *Physica* B, **256–258**, 490; 1999a, *Phys. Rev.* B, **60**, 11661.

Wójs, A., and Quinn, J. J., 1998, *Solid state Commun.*, **108**, 493; 1999a, *Solid state Commun.*, **110**, 45; 1999b, *Acta Phys. Pol.* A, **96** 403; 2000a, *Phil. Mag.* B, **80**, 1405; 2000b, *Phys. Rev.* B, **61**, 2846; 2001a, *Phys. Rev.* B, **63**, 045303; 2001b, *Phys. Rev.* B, **63**, 045304.

Wójs, A., Quinn, J. J., and Hawrylak, P., 2000a, *Phys. Rev.* B, **62**, 4630; 2000b, *Physica* E, **8**, 254.

Wójs, A., Szlufarska, I., Yi, K. S., and Quinn, J. J., 1999b, *Phys. Rev.* B, **60**, R11273.